BEAM LOSSES AND EMITTANCE GROWTH STUDIES AT THE RECORD HIGH SPACE-CHARGE IN THE BOOSTER

J. Eldred, V. Lebedev, K. Seiya, V. Shiltsev, FNAL, Batavia, Illinois, USA

Abstract

Comprehensive studies of high intensity proton beams in the 0.4-8 GeV FNAL Booster synchrotron have revealed interesting nonlinear dynamics of the beam losses and emittance growth at the record high $\Delta Q_{SC} = 0.6$. We report the results of the studies and directions of further improvements to prepare the Booster to the era of even higher intensity operation with new 0.8 GeV PIP-II linac.

BACKGROUND

In this document we describe out recent work towards a systematic, empirically-driven, up-to-date analysis of Fermilab Booster losses and emittance as a result of space-charge. We begin with careful consideration of instrumentation effects on aggregate Booster losses and within-cycle beam emittance. Next, we look at the dependence of beam loss and beam emittance on machine intensity. In [1] we have made a fuller presentation of this analysis and discuss other observed features of contemporary Booster operation. The data for this analysis was collected as part of a three-week international Booster collaboration event in June 2019 [2].

Our study of Booster performance is motivated by the near-term and long-term opportunity alike (see Table 1). Any insight into Booster loss and emittance growth mechanism thats lead to a realizable improvement of Booster operational performance, would provide an immediate benefit for the Fermilab HEP program. We also aim to prepare the Fermilab Booster for the upcoming PIP-II upgrade [3], which includes a new 0.8 GeV superconducting RF linac injector alongside a series of improvements to the Booster and Main Injector.

Our systematic study of the Booster at extreme space-charge presents a framework for the study of intense hadron rings more broadly. In the Fermilab context, there is a proposal for a new rapid-cycling synchrotron (RCS) [4, 5] to replace the Fermilab Booster as part of a 2.4 MW upgrade of the LBNF/DUNE program [6]. The space-charge loss model has a direct bearing on the minimum requirements for RCS injection energy and magnet aperture, as well as the projections for ultimate machine performance.

LOSSES

Aggregate Booster losses can be measured by declines in a toroid intensity monitor, although careful work was necessary to account for changes in the frequency response of the toroid as the machine ramps. With proper account of low-intensity losses, we believe the greatest operational concern are the intensity-dependent losses which take place over the first 8 ms. These losses are presented in Fig. 1. For this study the intensity is varied while other parameters are held fixed, the machine having been previously tuned for

Table 1: A Selection of Booster Parameters

Parameter		Value
Nominal intensity	N_p	4.3 e12
No. of injections		14 turns
Inj. (Extr.) energy	E_i	0.4 (8.0) GeV
RMS normalized emit	$\varepsilon_{x,y}$	2.0 π mm mrad
Ramp rate	f_0	15 Hz
Collimation efficiency	η	55%
Circumference	C	474.20 m
Max beta function	β_x, β_y	33.7, 20.5 m
Betatron tunes	ν_x, ν_y	6.75, 6.85
No. of cells, dipoles		24, 96
Gradient dipole structure		FOFDOOD
Harmonic number	h	84
RF frequency	f_{RF}	37.77-52.81 MHz
Max RF voltage	V_{RF}	1.1 MV
Transition energy	E_{tr}	4.2 GeV

regular operation with $4.5 \cdot 10^{12}$ protons. As one can see, the losses quickly grow with N_p – the solid line in Fig. 1 shows a cubic fit

$$\frac{\Delta N_p}{N_p} \approx 0.01 + 0.07 \cdot \left(\frac{N_p}{7 \cdot 10^{12}}\right)^3. \qquad (1)$$
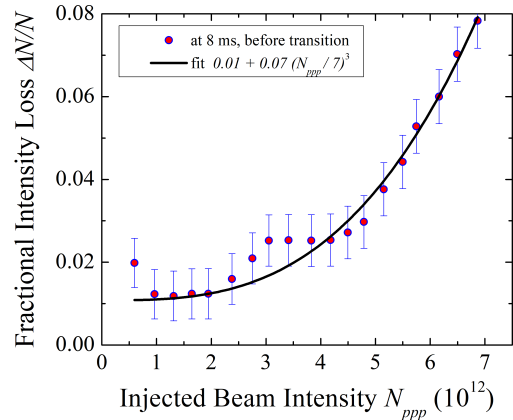

Figure 1: Intensity-dependent fractional Booster beam intensity loss at injection vs total number of protons.

In the absence of clearly detectable instabilities, we presume the cubic losses found in Eq. (1) are associated with space-charge. The incoherent space-charge tune-shift ΔQ_{SC} (neglecting pipe impedance) is a commonly used figure of merit for beam dynamics. This parameter ΔQ_{SC} [7] is given

by

$$\Delta Q_{SC} = \frac{N_p r_p B_f}{4\pi\varepsilon\beta_p\gamma_p^2}. \qquad (2)$$

Here N_p is the total intensity (assuming bunches fill all RF buckets), r_p is the classical proton radius, B_f is the bunching factor (the ratio of the peak to average bunch current), ε is the normalized rms beam emittance, and β_p and γ_p are relativistic Lorentz factors. The tuneshift is negative, but we omit the minus sign for simplicity. In operational circular rapid cycling accelerators, the space-charge parameter usually does not exceed 0.3-0.5 to avoid beam losses.

Taking the intensity dependence in Eq. (1) to arise from the intensity dependence of ΔQ_{SC} in Eq. (2) we write

$$\frac{\Delta N_p}{N_p} \propto \alpha\Delta Q_{SC}^{\kappa}. \qquad (3)$$

Here α is a machine-dependent constant and the space-charge scaling parameter κ is exponent. These parameters are empirical, and we leave it to future work to investigate the extent to which the scaling parameter $\kappa \simeq 3$ is specific to the Booster or generalizable to other machines.

We can consider a machine encountering a power limit W_{max} for uncontrolled losses, such as the typical 1 W per meter of machine circumference. For ΔN_p lost particles, the corresponding uncontrolled power loss W is given by

$$W = (1-\eta)f_0 \int E_k \delta N_p, \qquad (4)$$

where η is the collimator efficiency, f_0 is the cycle rate, and E_k is the kinetic energy of the lost particle. Under a power loss limit W_{max} we can then solve for the corresponding loss-rate

$$\frac{\Delta N_p}{N_p} = \frac{W_{max}}{(1-\eta)N_p E_k f_0}. \qquad (5)$$

From Eq. (3) and Eq. (5) we solve for the beam intensity corresponding to the space-charge loss-limit:

$$N_p^{max} \propto \left(\frac{W_{max}}{1-\eta}\right)^{\frac{1}{\kappa+1}} \left(\frac{\varepsilon}{B_f}\right)^{\frac{\kappa}{\kappa+1}} \frac{\gamma_p^{\frac{2\kappa-1/2}{\kappa+1}}}{(\alpha f_0)^{\frac{1}{\kappa+1}}}. \qquad (6)$$

One can immediately see that there are several paths to increase the space-charge intensity limit [8] and that this κ parameter determines the impact of those paths.

Let us examine the impact of three key changes for the PIP-II era Booster, taking $\kappa = 3$ from our loss measurements. With a new collimation units the Booster expects a 3-fold reduction fraction of losses which are uncontrolled (η from 55% to 85%) [9], corresponding to a $3^{1/4} \approx 33\%$ increase in N_p^{max}. With the PIP-II linac [3] the Booster injection energy will double (from 400 MeV to 800 MeV) and the combination of weaker space-charge with greater activation per lost particle should allow a 41% increase in N_p^{max}. Lastly, the Booster rep. rate f_0 will increase from 15 Hz to 20 Hz resulting in 7% reduction in the maximum intensity under a power loss limit. Altogether the 74% increase in the space-charge loss limit favors the 44% increase in intensity from

4.5·10¹² to 6.5·10¹² with some margin. Here, we neglect any further improvements to the beam distribution from PIP-II injection painting.

For rings at ultimate intensities, significant promise in loss reduction lies in improved beam dynamics that would make α and κ smaller, for example by injection "painting" to make the space-charge forces more uniform, by compensation of the most detrimental resonant driving terms (including enforcement of perfect periodicity in machine focusing optics), by space-charge compensation using electron lenses [10], or by implementation of the non-linear integrable optics [11]. For the latter two topics in particular, an R&D program is underway at the Fermilab IOTA facility [12].

EMITTANCE

The Booster measures beam size with ionization profile monitors (IPMs), which consists of a gated high voltage electric field and a micro-channel plate array. The IPM collects the residual gas ions generated by the passage of the proton beam, thereby imputing the beam profile.

In [13] a new physics-based model is used to calibrate Booster IPM data, bringing the IPM measure of emittance in the ring into accord with the multiwire measure of emittance in the extraction line. The model accounts for ion-drift effects which lead to an increase in uniform increase in apparent beam size and space-charge effects which lead to an increase in apparent beam size by charge density.

Having been calibrated for accuracy to ~ 10%, the IPMs can measure the beam emittance within the cycle. The resulting Booster IPM vertical beam emittance $\varepsilon_y(t)$ over the acceleration cycle is shown in Fig. 2 for a wide range of intensities N_p from 0.5·10¹² to 6.2·10¹².

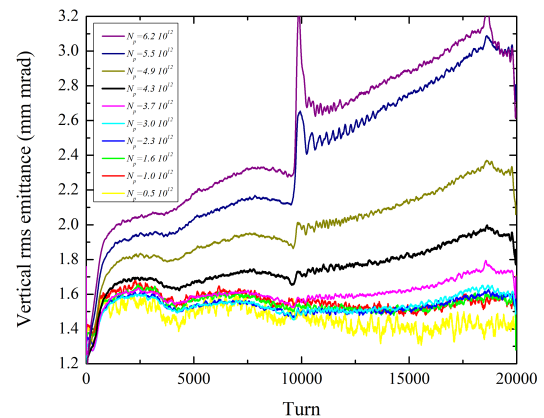Figure 2: Evolution of the IPM vertical emittance in the Booster cycle at different intensities N_p from 0.5·10¹² to 6.2·10¹². The operational intensity ($N_p = 4.3 \cdot 10^{12}$) is shown in the black. All the data are smoothed by a 100 turn running window averaging.

In general, the emittance evolution exhibits several features: i) fast growth over the first 2000-3000 turns; ii) steady growth for the rest of the cycle; iii) spikes at the time of transition and minor oscillations afterwards; and iv) 5-10%

variations at the end of the cycle. The last two effects are presumably instrumental.

Significant variation in the bunching factor at the transition is known to affect the IPM profile expansion [13]. Similarly, at the end of the acceleration cycle, the proton beam position in the IPMs varies over the last 2000 turns by as much as 6 mm in the horizontal plane and bunch rotation in the longitudinal phase-space prior the extraction at the very last hundreds of turns results in a smaller momentum spread and longer bunches.

We are interested in the first two effects, the rapid emittance growth after capture and the slow emittance growth during the ramp. Figure 3 shows how they depend on the beam intensity. The fast rms vertical emittance growth over the first 3000 turns is most probably due to record strong proton space-charge effects (see below) and scales approximately as:

$$\Delta\varepsilon_{y,3000}[\text{mm\,mrad}] \approx 0.17 + 0.61 \cdot \left(\frac{N_p}{7 \cdot 10^{12}}\right)^2. \quad (7)$$

One might contextualize the apparent quadratic intensity effect on emittance Eq. (7) with the apparent cubic intensity effect on losses Eq. (1) - as the beam size grows, and ever larger slice of the beam halo will either intercept a beam aperture directly or indirectly via an unstable region of multi-particle phase-space.

The slow emittance increase is roughly linear in time over the next 16000 turns, getts as big as 1 mm mrad (i.e. 30%) at $N_p = 6.2 \cdot 10^{12}$ and can be approximated as:

$$\Delta\varepsilon_{y,3000-19000}[\text{mm\,mrad}] \approx 1.85 \cdot \left(\frac{N_p}{7 \cdot 10^{12}}\right)^4. \quad (8)$$

Although a similar effect may have been seen in the Huang et al. 2006 IPM study [14], we have only recently begun to investigate the cause. A variety of hypotheses have been offered - an unaccounted for instrumentation effect, beam-induced vacuum activity, low-level RF noise, higher order resonances, collective effects and/or electron cloud effects. In support of the electron cloud effect, a ~15% reduction in the magnitude of this emittance growth was observed by using notching system to modify the bunch structure [15].

In Eq. (2) we gave an expression for the space-charge tuneshift parameter and discussed its role in driving losses. With the calibrated IPM data, combined with wall-current monitor data and the magnet ramp, we can calculate the vertical SC tuneshift parameter $\Delta Q_{SC}(t)$ in the Booster through out the ramp. Figure 4 shows the vertical SC tuneshift parameter $\Delta Q_{SC}(t)$ for just-above operational beam intensity $N_p = 4.6 \cdot 10^{12}$. The Booster space-charge tuneshift parameter peaks at about 1 ms after injection, and stays above 0.3 until about 6 ms (or 3000 revolutions). At the highest beam intensity studied $N_p = 6.2 \cdot 10^{12}$ the maximum space-charge tuneshift parameter ΔQ_{SC} peaks at $\simeq 0.75$

At operational and higher intensities, the incoherent space-charge tune spread does not fit between the half-integer
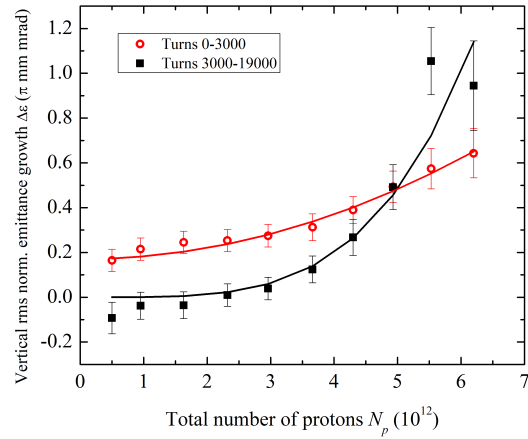

Figure 3: Vertical rms emittance growth vs N_p: (red circles) over the first 3000 turns; (black squares) from 3000 to 19000 turns. The error bars indicate estimated statistical uncertainty. Red and black solid line are for the approximations Eqs. (7) and (8), respectively.
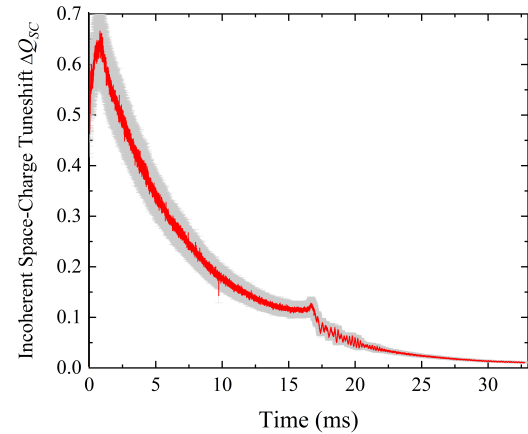

Figure 4: Calculated vertical space-charge tuneshift parameter for the Booster cycle with $N_p = 4.6 \cdot 10^{12}$. (Shaded area indicates 10% uncertainty, mostly due to the IPM emittance calculations).

($Q_y = 6.5$) and integer resonances ($Q_y = 7.0$). Tune-scans as a function of intensity confirm that the available tunespace with minimal losses and emittance growth shrinks to zero at operational intensities. There has been a reinvigorated effort to cancel the $2Q_y = 13$ half-integer resonance to improve Booster performance in the near-term, while managing the overall loss profile [16].

ACKNOWLEDGMENTS

REFERENCES

[1] J. Eldred, V. Lebedev, K. Seiya, and V. Shiltsev, "Beam intensity effects in Fermilab Booster synchrotron", *Phys. Rev. ST Accel. Beams*, vol. 24, p. 044001, 2021. `doi:10.1103/PhysRevAccelBeams.24.044001`

[2] J. Eldred *et al.*, "2019 Booster Studies Capstone Event", Fermilab, Batavia, IL, USA, Internal Note Beams-doc-7522, 2019.

[3] V. Lebedev *et al.*, "The PIP-II conceptual design report", Fermilab, Batavia, IL, USA, Technical Note FERMILAB-TM-2649-AD-APC, 2020.

[4] M. Syphers *et al.*, "An Upgrade Path for the Fermilab Accelerator Complex", Fermilab, Batavia, IL, USA, Technical Note TM-2754-AD-APC-PIP2-TD, 2021.

[5] J. Eldred *et al.*, "Versatile Multi-MW Proton Facility with Synchrotron Upgrade of Fermilab Proton Complex", Fermilab, Batavia, IL, USA, Letter of Interest SNOWMASS21-AF2_AF0-NF0_NF9_Jeffrey_Eldred-092, 2020.

[6] B. Abi *et al.*, "Deep Underground Neutrino Experiment (DUNE), Far Detector Technical Design Report, Volume II: DUNE Physics", Fermilab, Batavia, IL, USA, Technical Note FERMILAB-PUB-20-025-ND, 2020.

[7] J. Wei, "Synchrotrons and accumulators for high-intensity proton beams", *Rev. of Mod. Phys.*, vol. 75, p. 1383, 2003. `doi:10.1103/RevModPhys.75.1383`

[8] V. Shiltsev, "Fermilab proton accelerator complex status and improvement plans", *Mod. Phy. Let. A*, vol. 32, p. 1730012, 2017. `doi:10.1142/S0217732317300129`

[9] V. Kapin *et al.*, "Study of Two-Stage Collimation System in Fermilab Booster", Fermilab, Batavia, IL, USA, Internal Note Beams-doc-5519, 2017.

[10] V. Shiltsev, *Electron lenses for super-colliders*. New York City, NY, USA: Springer Publishing, 2015.

[11] V. Danilov and S. Nagaitsev, "Nonlinear accelerator lattices with one and two analytic invariants", *Phys. Rev. ST Accel. Beams*, vol. 13, p. 084002, 2010. `doi:10.1103/PhysRevSTAB.13.084002`

[12] S. Antipov, D. Broemmelsiek, D. Bruhwiler, *et al.*, "IOTA (Integrable Optics Test Accelerator): facility and experimental beam physics program", *J. Instrum.*, vol. 12, p. T03002, 2017. `doi:10.1088/1748-0221/12/03/T03002`

[13] V. Shiltsev, "Space-charge effects in ionization beam profile monitors", *Nucl. Instrum. Methods Phys. Res., Sect. A*, vol. 986, p. 164744, 2021. `doi:10.1016/j.nima.2020.164744`

[14] X. Huang, S. Y. Lee, K. Y. Ng, and Y. Su, "Emittance measurement and modeling for the Fermilab Booster", *Phys. Rev. ST Accel. Beams*, vol. 9, p. 014202, 2006. `doi:10.1103/PhysRevSTAB.9.014202`

[15] J. Eldred, "Preliminary Double-Notch Booster Ecloud Study", Fermilab, Batavia, IL, USA, Internal Note Beams-doc-891, 2020.

[16] J. Eldred, "Analysis of IPM Data for Booster Half-Integer Study", Fermilab, Batavia, IL, USA, Internal Note Beams-doc-8935, 2021.